

## ABSTRACT

Title of Thesis:

IN-SITU ELECTRO-ASSEMBLY OF REDOX-BASED GLUCOSE SENSORS FOR MICROFLUIDIC APPLICATIONS

Joanne Chan, Chandni Dhamsania, Monil Ghodasra, Elana Laster, Kimberly Lo, Julie Mehta, Mayuri Patel, Veda Ravishankar, Sam Rombro, Yasas Santharam, Sarah Onimus, Joy Wang, Jessica Yau

Thesis directed by:

Dr. William E. Bentley, Fischell Department of Bioengineering

Microfluidic models of the gastrointestinal (GI) tract, known as gut-on-a-chip devices, mimic the structural, absorptive, pathophysiological and microbial environment of the human gut. They have potential to revolutionize drug delivery testing and replace animal testing to improve efficacy. However, current models lack methods for quantitative assessment of molecular cues that determine biological function, limiting their ability to discern the efficacy of treatments on diseases. Team BioCHIPS developed a polydimethylsiloxane (PDMS) gut-on-a-chip model lined with Caco-2 intestinal epithelial cells, with the novel incorporation of catechol-chitosan biomolecular sensors. This is the first instance of *in situ* assembled biomolecular sensors that provide direct electrical connectivity and assessment of glucose level in real time. These sensors enable quantifying changes in the physiological conditions due to alterations in glucose concentration, to monitor effects of treatments on their respective GI diseases.

IN-SITU ELECTRO-ASSEMBLY OF REDOX-BASED GLUCOSE SENSORS FOR  
MICROFLUIDIC APPLICATIONS

By

Team BioCHIPS

Joanne Chan, Chandni Dhamsania, Monil Ghodasra, Elana Laster, Kimberly Lo, Julie  
Mehta, Mayuri Patel, Veda Ravishankar, Sam Rombro, Yajas Santharam, Sarah Onimus,  
Joy Wang, Jessica Yau

Thesis submitted in partial fulfillment of the requirements of the  
Gemstone Honors Program, University of Maryland,  
2018

Advisory Committee:

Dr. William E. Bentley (Chair)

Mr. Wu Shang

Dr. Ryan D. Sochol

Dr. Gregory F. Payne

Dr. Xiaolong Luo

Ms. Nedelina Tchangalova, Team Librarian

## Acknowledgements

We would like to thank Dr. William E. Bentley for his mentorship and inspiration since the initial project proposal; our junior mentor, Wu Shang, for his patience and guidance throughout these three years; and Dr. Gregory F. Payne for providing his lab space. We would also like to acknowledge the help of John Abrahams and the staff of Fablab, the staff of Dr. Bentley and Dr. Payne's Lab, the staff of Terrapin Works, and all the professors and experts who trained and assisted us with technical skills.

Thank you to the Gemstone Staff, Dr. Frank Coale, Dr. Kristen Skendall, Vickie Hill, Leah Kreimer, and Jessica Lee for keeping us on track, encouraging us, and providing us with invaluable resources. Thank you to our Librarian, Nedelina Tchangalova, for her guidance on all things literature review and written. Finally, thank you to our family, friends, and LaunchUMD donors for financial and moral support.

## Table of Contents

<b>Chapter 1: Introduction</b>	<b>6</b>
<b>Chapter 2: Literature Review</b>	<b>8</b>
<b>2.1 Gut-on-a-Chip</b>	<b>8</b>
2.1.2 Applicability to OoC Model	10
2.1.3 Gut-on-a-Chip Characteristics	11
2.1.4 Current Research on Gut-on-a-Chip	13
<b>2.2 Fabrication</b>	<b>14</b>
2.2.1 Materials for Fabrication	14
2.2.2 Biofabrication & Soft Lithography	16
2.2.3 Fabrication of Internal Microenvironment	17
2.2.4 Three-Dimensional Printing	17
<b>2.3 Sensors</b>	<b>18</b>
2.3.1 Potential Sensor Options	18
2.3.2 Catechol-Chitosan Redox Sensor	19
<b>2.4 The Disease: <i>Clostridium difficile</i> Infection</b>	<b>21</b>
2.4.1 Impact of Infection	21
2.4.2 Potential Treatment Methods	22
<b>2.5 Treatment of Interest</b>	<b>24</b>
2.5.1 Vancomycin	24
2.5.2 Advantages and Disadvantages of Vancomycin	24
2.5.3 Recolonization after Antibiotic Treatment	26
<b>Chapter 3: Methodology</b>	<b>27</b>
<b>3.1 Objectives</b>	<b>27</b>
<b>3.2 The Gut-On-A-Chip</b>	<b>27</b>
3.2.1 Chip Component Design	27
3.2.2 Fabrication of the Chip	29
3.2.3 Fabrication of the Gold Electrode	30
3.2.4 Three-Dimensional Printing Microvilli	31
<b>3.3 Cell Studies</b>	<b>32</b>
3.3.1 Preliminary Caco-2 Cell Culture	32
3.3.2 Implantation of Caco-2 cells into gut-on-a-chip model	32

<b>3.4. The Sensors</b>	<b>33</b>
3.4.1 Electrodeposition Solution Preparation	33
3.4.2 Electrodeposition	33
3.4.3 Sensor Testing	35
<b>Chapter 4: Results</b>	<b>37</b>
<b>4.1 Creation of the Gut Microenvironment</b>	<b>37</b>
<b>4.2 Integration of Gold Electrode Sensors</b>	<b>38</b>
<b>Chapter 5: Discussion</b>	<b>41</b>
<b>5.1 3D Printing of the Microvilli Structures</b>	<b>41</b>
<b>5.2 Biofabrication of an alternative PDMS gut-on-a-chip model</b>	<b>42</b>
<b>5.3 Integration of gold electrode sensors</b>	<b>43</b>
<b>Chapter 6: Conclusion</b>	<b>45</b>
<b>References</b>	<b>47</b>

## Chapter 1: Introduction

According to the National Center for Advancing Translational Sciences (NCATS), more than 30 percent of promising medications have failed in human clinical trials, despite positive results from animal trials.<sup>1</sup> It is difficult to determine whether a medication is safe for humans through animal testing and is even more difficult to obtain approval for the distribution of the medication.<sup>2</sup> The United States Food and Drug Administration (FDA) estimates that it takes about ten months for a ‘Standard Review’ of new drugs that offer minor improvements for existing therapies and six months for ‘Priority Review’ drugs that are major advances in both existing and non-existing treatments.<sup>3</sup> While the timeline proposed by the FDA is ideal in principle, the process can extend to over five years and is followed by four phases of clinical trials, which can add several years to the timeline.<sup>3</sup> The process to research and develop a typical drug takes, on average, 7.3 years and \$650 million.<sup>4</sup> The resulting process of research and development is not only time consuming, but also expensive.<sup>4</sup> These factors severely limit the development and availability of new drugs, particularly those that might have limited markets.

*In vivo* and *in vitro* laboratory techniques are the most commonly used platforms for disease modeling and drug and chemical testing.<sup>5</sup> Although they have been able to provide information about the effects of the drug in physiological conditions, they present several drawbacks. *In vivo* models can produce integrated multi-organ responses to experimental substances; however, multi-organ systems that may seem advantageous create difficulties when trying to pinpoint specific physiological and pathological responses to a particular cell group.<sup>5</sup> In addition, applying animal model data to human conditions are limited because animals have different physiological responses and

anatomical features compared to humans.<sup>6</sup> These differences can lead to the failure to adequately mimic clinical diseases or cause publication bias, where the publication of results depends on the hypothesis being tested, and the significance of the results depends on the quality of the research.<sup>7</sup> On the other hand, *in vitro* platforms are useful for studying the molecular basis of physiological and pathological responses, such as identifying the proteins, genes, and other components involved, but they can fail to simulate complex cell-cell and cell-cell matrix interactions.<sup>8</sup>

The limitations of the traditional models have led to the failure of a number of new drug candidates throughout various testing phases due to unexpected side effects or low efficiency.<sup>9</sup> To overcome these limitations, scientists are looking into a new way to test drugs and model diseases: organ-on-a-chip models (OoC). OoC models are microchips created by coating glass slides with human cells to imitate a specific organ.<sup>10</sup> Current research of OoC models focus on modeling the structure and function of human organs and systems on a microfluidic device, creating a “newer human cell based approach.”<sup>1</sup> With this approach, pharmaceuticals can be efficiently tested without animal or human test subjects. The chip would allow for a faster drug screening process, which will ultimately benefit pharmaceutical and biomedical research companies as well as the public.

This research focuses on the gastrointestinal tract to create a gut-on-a-chip model integrated with sensors. The sensors will provide a more quantitative analysis by measuring the quantitative effect of a potential treatment on a disease. If sensors can be successfully integrated into the gut-on-a-chip model, then treatments can be more accurately tested and modeled for their respective diseases.

## Chapter 2: Literature Review

### 2.1 Gut-on-a-Chip

#### 2.1.1 The Gastrointestinal Tract

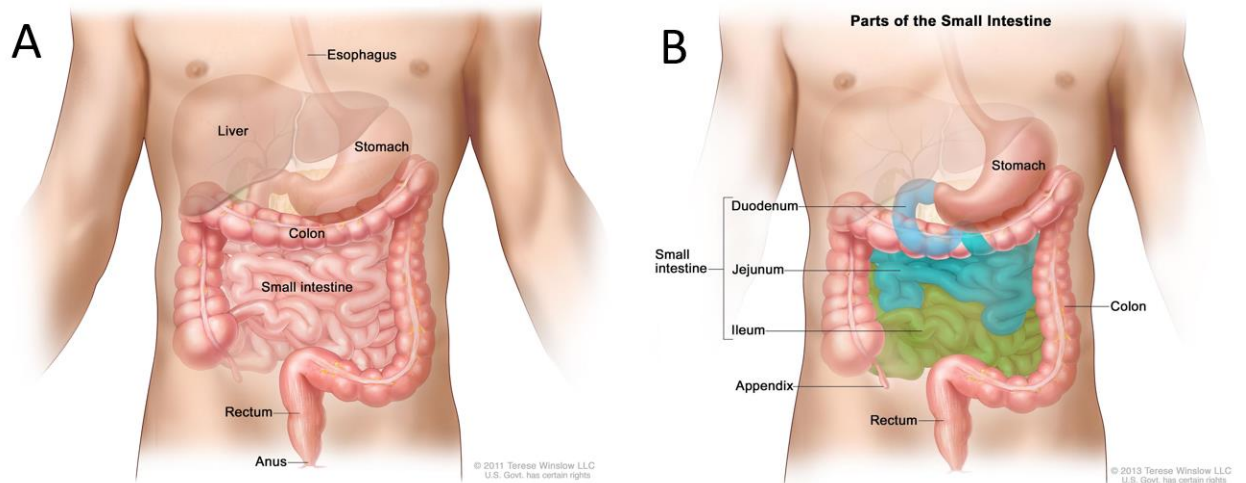
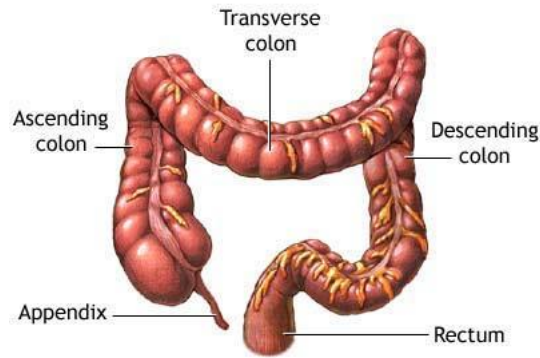


**Figure 2.1** (A) *Depiction of the parts of the gastrointestinal tract*<sup>11</sup> (B) *Depiction of the parts of the small intestine*<sup>12</sup>

The gastrointestinal (GI) tract (Figure 2.1A) is an organ system in the body composed of the stomach, small intestine, and large intestine.<sup>13</sup> This research will focus on both the small and large intestines, commonly known as the gut.

The small intestine is about 6 m long and very tightly folded (Figure 2.1B).<sup>14</sup> It is a long, tube-like structure made up of three segments: duodenum, jejunum, and ileum.<sup>15</sup> These sections carry semi-digested food from the stomach through a process of further digestion where nutrients are absorbed while the leftover waste travels to the large intestine. The small intestine most notably contains numerous villi, which are approximately 500  $\mu\text{m}$  in length, as well as tight-junctions between the cells.<sup>16</sup> The villi are hair-like structures that increase the inner surface area, which, in combination with the tight junctions, result in an increased efficiency of nutrient absorption.





ADAM.

**Figure 2.2** Depiction of the parts of the large intestine<sup>17</sup>

The large intestine, also known as the colon, is only 1.5 m long, but slightly wider in diameter than the small intestine, which is why it is known as the larger one of the intestines (Figure 2.2).<sup>18</sup> The colon is also made up of three segments: ascending, transverse and descending.<sup>17</sup> When the digested food passes through the small intestine, it empties out into the large intestine. The colon reabsorbs water and pushes the food waste towards the rectum. The rectum collects leftover waste until it is emptied through the anus.<sup>13</sup>

One of the most important characteristics of the intestinal system is its microbiome and its associated microbiota. The intestinal microbiome refers to the collection of microorganisms that occupy a specific environment, while the microbiota is in reference to the actual microorganisms.<sup>17</sup> The environment of the intestine has a dynamic pH depending on location. As a result, the species of bacteria differ based on the local conditions. Both play an important role in the development and function of the gastrointestinal structure.<sup>17</sup> The microbiome contains both beneficial and detrimental kinds of bacteria.<sup>17</sup> The beneficial bacteria, such as *Lactobacillus*, are ingested and aid in the human digestive process.<sup>17</sup> Detrimental bacteria, such as *Clostridium difficile* and certain strains of *Escherichia coli*, are also essential for digestive processes, but can cause harmful

diseases if humans are exposed to them from external sources in large amounts.<sup>17</sup> Both types of bacteria are vital to the function of the human gut. According to a study conducted by Abrams, Bauer, and Sprinz, rats grown in germ-free conditions exhibited reduced intestinal surface area and decreased epithelial cell turnover.<sup>19</sup> These morphological differences lead to a less effective intestinal system and GI functional disorders.<sup>20</sup> Nevertheless, in the case of overgrowth, bacteria can produce toxins and increase the permeability of the gut membrane, also resulting in harmful diseases.

### **2.1.2 Applicability to OoC Model**

Developing *in vitro* models of the human gut plays a key role in addressing challenges with GI tract diseases, metabolism, transport, and oral absorption of drugs and nutrients. These cell culture models contain a transepithelial barrier that can study the fluid and transport properties of cells.<sup>21</sup> Current *in vivo* methods for toxicity evaluation of drugs are impractical for the GI tract due to the large experimental scale and the immunological differences between species used in animal studies and human cell culture.<sup>22</sup> These obstacles need to be overcome because the gut is one of the most important organ systems, as it contains major mechanisms for the digestion and absorption of nutrients needed for bodily functions. In addition, the gut can be targeted for drug delivery since it contains its own microbiome, which controls important processes that maintain the immune system. On the other hand, the gut is difficult to replicate due to the harsh acidic environment and varying pH ranges from the proximal end of the colon to the cecum, the junction of the small and large intestine.<sup>23</sup> The thin mucous layer adds complexity due to its  $\mu\text{m}$  size. Furthermore, the tight junctions prevent highly charged and large molecules from entering

the GI tract. Thus, conducting research on the GI tract and its diseases presents its own unique set of obstacles.

Despite these limitations, the gut was chosen for this OoC model because it has its own microbiome, which makes it independent. Compared to an organ that is completely integrated into the human body and whose functions depend on other organs, the isolation of the gut provides an optimal testing area. The human gut-on-a-chip model is able to accurately present the three-dimensional (3D) structures, differentiated cell types, and physiological functions of the GI tract, thereby providing an alternative *in vitro* model to study intestinal diseases and drug development.<sup>24</sup> This model can simulate fluid flow, mechanical stress, epithelial cell behavior, and transfection potential of the gut to monitor nanoparticle transport and drug delivery in real time using imaging techniques such as confocal microscopy and flow cytometry. Different concentrations and conditions can be researched and trialed to rapidly test the drug delivery system. Moreover, 3D cell cultures are more advantageous than two-dimensional (2D) cell cultures. A study done by Carrel et al. concluded that cells that were three-dimensionally cultured had a longer life span.<sup>25</sup> In order to ensure that life span, a constant supply of nutrients to the cells and the removal of metabolites are needed to allow the 3D structure to grow properly.<sup>26</sup>

### 2.1.3 Gut-on-a-Chip Characteristics

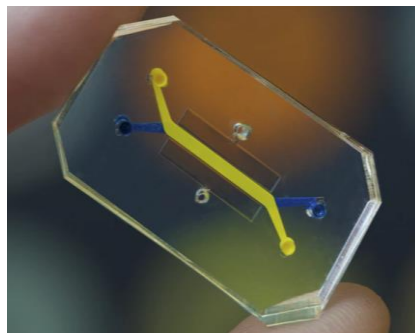


**Figure 2.3** Gut-on-a-Chip model by Yu et al. at Wyss Institute<sup>27</sup>

Yu et al. developed a microfluidic device that has a single layer of human intestinal epithelial cells that grow on a flexible, porous membrane inside the central chamber, recreating the intestinal barrier.<sup>27</sup> This device (Figure 2.3) exhibits a cyclic mechanical deformation that mimics the peristaltic, or wave-like, motions that move along the digestive tract. An important characteristic of this gut-on-a-chip model is the intestinal tissue-tissue interface, which allows fluids to flow through the cell layer. Additionally, this model is able to grow and sustain common intestinal microbes on the surface of the cultured intestinal cells. Gut-on-a-chip models successfully simulate the physiological properties that are important in understanding intestinal diseases and drug testing.<sup>24</sup>

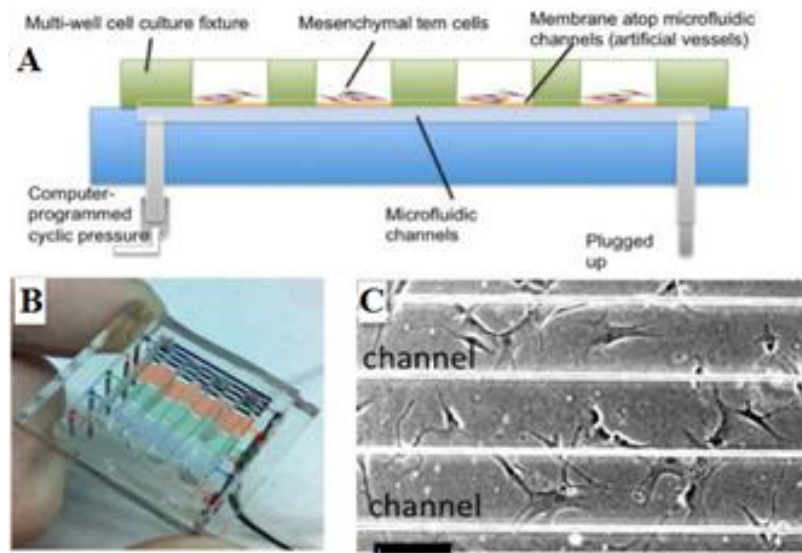


**Figure 2.4** A) Schematic depiction of fully packaged microfluidic culture system. B) Photograph of a packaged microchip. C) Human mesenchymal vessels for dynamic mechanical stimulation of mesenchymal cells cultured on two microfluidic vessels. (Scale bar = 200  $\mu\text{m}$ )<sup>28</sup>

Another important aspect of OoC models is the microfluidic system that acts as a pathway for miniscule amounts of liquids (Figure 2.4). Microfluidic systems simulate blood vessels, a network of tubes that allows blood to circulate within the body. When drugs are ingested, internal organs absorb and transport them throughout the body via blood vessels. Due to the crucial role blood vessels play in drug delivery, microfluidic systems

are imperative to developing a viable OoC. A key principle of the microfluidic system is fluidic shear stress, which is when fluid particles move relative to one another at different velocities. Concepts such as peristaltic movement, chemical gradients, and cell-cell communication are also integrated into the final design of the model. Researchers are able to conduct parametric studies when these factors are monitored and managed.

#### **2.1.4 Current Research on Gut-on-a-Chip**

The current model, with its similarities to the human gut allows researchers to test novel drug delivery techniques. Drug delivery techniques have evolved from drug-loaded nanoscale liposomes to polymeric nanoparticles that can be chemically modified for *in vivo* stability to target a disease.<sup>21</sup> Vacuum channels, pressurized to mimic peristalsis, are combined with the diverse microenvironment, which uses epithelial cells on hydrogel substrates to replicate the lining of the GI tract and test the development of intestinal disorders.<sup>20</sup> Using this model, further studies could be done on metabolism, absorption of drugs and chemicals, and an assortment of diseases.

With this model, Gamboa and Leong were able to test a nanoparticle-mediated delivery system that can minimize the degradation of the cargo, extend the retention time in the gut, and enhance transport to the systemic circulation. Yu et al. improved the model by designing a 3D villous model that showed how villous scaffolds facilitate cell differentiation and absorption.<sup>27</sup> The villous scaffolds allow for transport away from cells in a basolateral direction, while hard surfaces do not permit transport through the cell monolayer.<sup>29</sup> Costello et. al. found that in the gut-on-a-chip model with liquid shear, there was also increased cell proliferation and more active (as opposed to passive) glucose

transport at higher rates under flow.<sup>30</sup> This is favorable to the 2D model by creating a more accurate representation of the microbiota in the gut.

Another study used droplet microfluidics, a tool that allows for the use of miniscule (pico- to nano-liters) amounts of sample for low cross-contamination and faster mixing.<sup>26</sup> Droplet formation can be controlled by hydrodynamic and electro-hydrodynamic properties of a particular channel. These properties relate to the study of uncharged and charged fluids in motion, such as flow rate, pressure, density, and temperature. Electro-hydrodynamics involves integrating electrodes that transmit an electrical signal to control the formation of the droplets.<sup>26</sup> This study can be combined with the gut-on-a-chip system to improve drug delivery.

## **2.2 Fabrication**

### **2.2.1 Materials for Fabrication**

As microfluidic devices are becoming powerful tools in the realm of biological, chemical, and medical analysis, materials like glass, silicon, plastics, hydrogels, and elastomers have been introduced and utilized in biofabrication. Finding and implementing the balance between the effectiveness of the material, ease of fabrication, and cost has been one of the challenges researchers face in the development of the OoC model.

Plastics have become a popular option due to their rapid prototyping potentials at a low cost and high flexibility to meet the researchers' needs.<sup>31</sup> Thermosets, such as SU-8 photoresist and polyimide, can withstand high temperatures, resist various solvents, and are optically transparent.<sup>31</sup> An optically transparent chip would allow for inverted phase contrast microscopy of the culture and measurement at all times.<sup>32</sup>

Polymers or elastomers are the most popular material for microfluidic chip fabrications.<sup>31</sup> The advantages of elastomers include low cost, rapid and simple prototyping, and properties that allow for complicated and parallel fluidic microfabrication in channel structures and cultures.<sup>31</sup> The cross-linked polymers chains stretch and compress with external forces, which will allow these OoC models to more accurately prototype external forces on the system.<sup>31</sup> Polydimethylsiloxane (PDMS) is commonly integrated into the fabrication of microfluidic devices. Due to its low surface tension, researchers can easily peel templates from a mold and seal them to other pieces of PDMS, glass, and substrates.<sup>31</sup> The gas permeability of PDMS allows the surface of the device to be compatible for cell cultures in OoC models.<sup>31</sup> Although PDMS seems to be the ideal material for microfluidics, researchers must take into account that PDMS is insoluble with organic solvents, thus restricting it to aqueous solutions.<sup>31</sup> In addition, quantitative experiments using PDMS are not as reliable since researchers have found that it absorbs small hydrophobic molecules and biomolecules, such as carbohydrates.<sup>29</sup>

Yet another option is hybrid and composite material, which combine at least two of the common materials. PDMS and glass are typically used for research labs while plastic is used for commercial devices.<sup>31</sup> The combination of PDMS with other materials has proven successful in gut-on-a-chip models in laboratories at the University of Maryland.<sup>33</sup> Current gut-on-a-chip models are fabricated via soft lithography, which shapes PDMS on a mold with microchannel patterns on a silicon wafer with negative photoresist SU 8, a thermoset.<sup>33</sup>

### **2.2.2 Biofabrication & Soft Lithography**

Biofabrication has recently been introduced as a way to construct imitations of biological products in fluidic systems with minimal instrumentation.<sup>33</sup> It utilizes additive manufacturing, also known as 3D printing, for tissue engineering from cells, gels, and other biomaterials.<sup>34</sup> Photolithography is the most dominant and powerful technique used in microfabrication, a subset of biofabrication. It is a parallel process and allows for the production of patterned structures in thin films of photoresists with features as small as approximately 250 nm. Although photolithography can also be used for creating larger  $\mu\text{m}$ -scale features, it is not cost effective, allows no control of the chemistry of the surface, and is limited to use with a small set of photosensitive materials.<sup>35</sup>

An extension to photolithography is soft lithography, which uses replica molding of nontraditional elastomeric materials to fabricate PDMS blocks or stamps and microfluidic channels.<sup>36</sup> An elastomeric block, commonly PDMS or, in some cases, silicone rubbers, with patterned relief structures on its surface is the main element of soft lithography. A prepolymer of the elastomer is poured over a master having the relief structure on its surface, which is then cured and peeled off.<sup>35</sup> Once cured PDMS is delaminated from the mold, which can then be bonded to glass slides by oxygen plasma treatment.<sup>31</sup>

Soft lithography offers many advantages in producing a variety of functional components and devices. It can be utilized in areas ranging from optics to microanalysis to display to microelectromechanical systems (MEMS), to microelectronics. It serves as an optimal fabrication method for constructing a microfluidic device such as the gut-on-a-chip model. Soft lithography also allows for fabrication of complex, optically-functional surfaces, and functional microelectronic devices in order to accommodate circuitry.<sup>32</sup> This



technique is the prominent fabrication method for OoC models because it illustrates the advantage of flexibility in terms of extending micropatterning into dimensions, materials, and geometries.<sup>32</sup>

### **2.2.3 Fabrication of Internal Microenvironment**

The microenvironment of the gut-on-a-chip model will consist of two components: human cells and bacteria that make up the microbiome of the intestines. Caco-2 cells are a continuous cell line of heterogeneous human epithelial colorectal adenocarcinoma cells derived from the colon carcinoma.<sup>37</sup> They can be differentiated and polarized to be phenotypically, morphologically, and functionally similar to enterocytes.<sup>37</sup> Additionally, Caco-2 cells can undertake transepithelial ionic transport and can express small intestine microvilli hydrolases and nutrients transporters, microvilli and tight junctions.<sup>37</sup>

### **2.2.4 Three-Dimensional Printing**

Three-dimensional (3D) printing, also known as additive manufacturing, is a recent and growing interest in the realm of microfluidic devices. Traditional lithography requires extensive external equipment to regulate the internal functions of the microfluidic chips. To address this limitation, 3D printing shows potential in printing microfluidic circuitry. The general approach to fabricate 3D structures includes extrusion-based deposition, stereolithography (SLA), and multijet modeling (MJM).<sup>38</sup> The extrusion-based or nozzle-based techniques are usually used to create sub-millimeter scale cellular constructs and are primary methods of 3D printing.<sup>38</sup> SLA has been used to fabricate resistor link components that are useful in microdroplet generation and even cell culture at the hundreds of microns resolution. SLA can only support one material being printed, thus limiting the use of sacrificial material for supports in complex structures.<sup>38</sup> MJM, however, allow for tens of

microns resolution and the printing of numerous materials simultaneously.<sup>34</sup> This is a valued aspect of MJM, and in recent years, has been examined from the static and dynamic perspective.<sup>39</sup> The advances of additive manufacturing have huge potential in the fields of OoC fabrication.

## **2.3 Sensors**

### **2.3.1 Potential Sensor Options**

A primary focus of this research will be different types of sensors and how they can be manipulated to sense biological molecules. Biochemical properties such as temperature, pH, and oxygen levels can be measured using two types of sensors. Amperometric oxygen sensors can detect oxygen concentrations as the surrounding electrical current changes. There are also chemo-sensors, which can measure ion concentrations such as potassium, sodium and chloride.<sup>40</sup> Two types of chemo-sensors, ion-sensitive field-effect transistor (ISFET) sensors and chemical field-effective transistor (CHEMFET) sensors, have many different applications in medicine and biomedical research. Some of the many applications include a penicillin sensor, urea detector and glucose sensor. ISFET sensitivity is dependent on the gate dielectric material, which usually consists of silicon and metal oxides or nitrides. While ISFETs can only detect hydrogen ions, CHEMFETs possess the technology to detect other ions.<sup>41</sup> These sensors provide perfunctory quantitative measurements, but pH and temperature will be held constant in the gut-on-a-chip model in order to reduce confounding variables, rendering these sensors nonessential.

Nanostructured microelectrodes (NMEs) have been used in the past for the sensitive detection of nucleic acids, proteins, and small molecules. Their high sensitivity makes them

ideal for applications in which small sample volumes are desirable.<sup>42</sup> However, NMEs that detect small molecules relevant to *C. difficile* or vancomycin do not exist. To create an entirely new class of sensors would not be feasible with the limited amount of time and resources available.

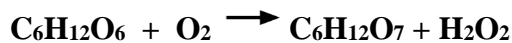
Yet another type of sensor that can be used is a magnetic cell-based sensor. Conventional sensors generally use chemical, optical, spectroscopic, electrical impedance- or mass-based detection to interpret biochemical phenomena. Cell-based sensing makes use of living cells or tissues as an integral part of the sensor and utilizes inherent cellular mechanisms to perform accurate detection of cell- or tissue-specific responses. This type of sensor can provide high sensitivity and specificity. Depending on the application of interest, the magnetic cell-based sensor can be outfitted with a variety of cell types with diverse functionalities. Such a sensor can be used to detect any range of biochemical agents.<sup>43</sup> Despite these advantages, this sensor is not easily adaptable to different applications. For every target molecule, a new sensor would have to be created. Moreover, the fabrication of such sensors would be convoluted, as this technology is novel and not very well understood yet. This research requires established and reliable sensors to integrate in the model. Similar to the ISFETs and CHEMFETs, limited time and resources do not allow for this.

### **2.3.2 Catechol-Chitosan Redox Sensor**

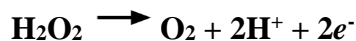
To assay biomolecules, one can typically use mass spectroscopy or chromatography or various “omics” methodologies. All of these methods require the researcher to take a sample, treat the sample, and subject it to a large, off-line, analytical method. On the other hand, biology offers the ability to detect biology. Enzymes can be

used to recognize and quantify the level of enzyme substrates. Enzymes, however, cannot be assembled into microfluidic devices during the construction of the device. Lithography and PDMS molding use high temperatures and toxic materials that do not allow for the incorporation of biological entities to be assembled within the devices. Further, biological entities that are incorporated into devices are stable for relatively short periods of time. Using a catechol-chitosan sensor offers a method to incorporate the enzyme into the device near where the measurement is needed and at a time near when the measurement is needed. Chitosan is ideal for its weak polyelectrolyte properties as it is deprotonated and soluble at low pHs and protonated and insoluble at high pHs.<sup>44</sup> Its approximate pKa of 6.5 is in the ideal range for biological applications. Chitosan's pH responsive film-forming properties allow it to yield 3-D hydrogel networks.<sup>45</sup> To create the sensor, chitosan is electrodeposited onto a gold electrode, which would then be able to measure electric potentials caused by redox reactions.<sup>38</sup> Gold is used in biomedical applications due to its biocompatibility. Other metals, like platinum and iridium are easily oxidized, while gold is much more stable. It is also a better conductor than aluminum, copper and silver.<sup>44</sup> Anodic electrodeposition is used to create the film on the gold electrode. Particles (GOx) that are dissolved in a liquid medium (chitosan) migrate towards the metal using an electric field and are deposited in a stable film onto the electrode.<sup>46</sup> The thickness of the film is dependent on the duration of deposition. Anodic deposition is chosen over cathodic because it allows for a more durable film. A film created by cathodic deposition would require layer-by-layer assembly in order to ensure imperishability. Anodic deposition allows for a one-step method for electrodepositing the chitosan solution.<sup>47</sup>

While this sensor can only detect for redox-active molecules, non-redox-active molecules can still be detected by reacting them with other redox-active molecules. For example, in order to detect glucose concentration, glucose oxidase (GOx) can be added to facilitate the reaction between glucose and oxygen, which forms gluconic acid and hydrogen peroxide (H<sub>2</sub>O<sub>2</sub>) while oxygen concentration is held constant as shown in Equation 2.1. The H<sub>2</sub>O<sub>2</sub> will subsequently apply a current to the electrode as shown in Equation 2.2, which will allow for detection of the molecule. The concentration of H<sub>2</sub>O<sub>2</sub> will be used to extrapolate the unknown glucose concentration using Equation 2.1.



**Equation 2.1** In this equation glucose (C<sub>6</sub>H<sub>12</sub>O<sub>6</sub>) is reduced using oxygen (O<sub>2</sub>) to create gluconic acid (C<sub>6</sub>H<sub>12</sub>O<sub>7</sub>) and H<sub>2</sub>O<sub>2</sub>.



**Equation 2.2** In this equation H<sub>2</sub>O<sub>2</sub> is oxidized to create O<sub>2</sub>, protons (H<sup>+</sup>), and electrons (e<sup>-</sup>).

## 2.4 The Disease: *Clostridium difficile* Infection

### 2.4.1 Impact of Infection

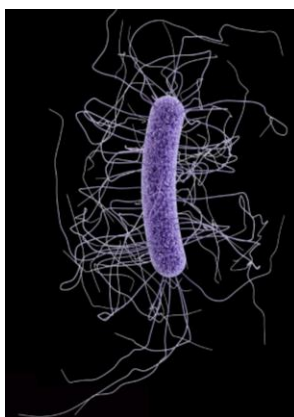


**Figure 2.5** *Clostridium difficile* <sup>48</sup>

According to a study released by the Center for Disease Control and Prevention (CDC), every year, approximately half a million patients in the United States are infected

by a fatal, rod-shaped bacterium called *Clostridium difficile* (Figure 2.5).<sup>45</sup> This bacterium causes the colon to be inflamed, which leads to extreme and, possibly, fatal diarrhea. *C. difficile* infection is a contagious disease that can be spread orally. It has been noted that 29,000 patients die within one month of being diagnosed with the infection and, of those people, about 15,000 die as a direct result of CDI treatment.<sup>49</sup> In fact, over the years, it has become the leading cause of microbial healthcare-associated infections in U.S hospitals. Currently, about 76 percent of CDI's occur in hospital patients, a large proportion of which are diagnosed within two months of receiving antibiotics.<sup>50</sup> Once contracted, the disease can be so severe, it often forces patients to extend their hospital stay by an average of 21 days.<sup>51</sup>

Moreover, people who are taking antibiotics are at the highest risk for developing CDI. When patients are prescribed several antibiotic treatments concurrently, beneficial bacteria in the gut can be suppressed or harmed. Without these benign bacteria in the body, the rapid growth of *C. difficile* can lead to serious consequences. The bacteria produce toxins that destroy cells in the lining of the intestine and produce plaques of inflammatory cells. Ultimately, the cellular debris inside the colon decays and causes watery diarrhea.<sup>49</sup>

#### **2.4.2 Potential Treatment Methods**

One of the most common treatments for CDI is vancomycin, which attacks the most severe forms of the disease. Other, more novel treatments, such as fecal microbiota transplantation (FMT), are now being studied as well. Microbiota transplantation involves eradicating the bacteria from an infected gut and replacing it with a whole new microbiota via fecal transplant or a fecal matter pill. The FDA has recently classified FMT as an

investigational new drug for treating *C. difficile* infection which is unresponsive to standard therapies, which signals a promising future for FMT treatment.<sup>52,53</sup>

Initial treatment for CDI involves discontinuing the use of offending antimicrobials. Historically this was able to resolve symptoms for 20 to 25 percent of patients within 48 to 72 hours.<sup>49</sup> However, due to the evolution of more pernicious strains, delaying the administration of specific therapeutic measures is not advised. The most common treatments for CDI are vancomycin and metronidazole. These antibiotics need to be introduced into the colonic lumen where the *C. difficile* is located, and toxins that result in colitis symptoms are produced.<sup>54</sup> Between 1977 and 1980, most physicians prescribed oral vancomycin to treat confirmed cases of CDI. In the early 1980s, metronidazole was found to be just as effective as vancomycin.<sup>55</sup>

Oral vancomycin serves as the prime antibiotic in CDI treatment. As low levels of the drug are absorbed, there are virtually no serum levels, and colonic levels are very high.<sup>54</sup> Vancomycin was first sold in the 1950's and later approved officially for use by the U.S. Food and Drug Administration (FDA). This resulted in vancomycin becoming the standard treatment for colitis. In the past 20 years, alternative treatments for CDI such as bacitracin, fusidic acid, and teicoplanin have emerged; however, vancomycin and metronidazole have surfaced as top candidates for treatment as selected by clinicians of the field.<sup>54</sup> Given metronidazole's high absorptivity in the small bowel, vancomycin has since been recognized as a superior treatment.

## 2.5 Treatment of Interest

### 2.5.1 Vancomycin



**Figure 2.6** Front and back images of 250 mg tablets of vancomycin<sup>56</sup>

Vancomycin (Figure 2.6) is a glycopeptide antibiotic synthesized by the *Amycolatopsis* genus. It consists of the sugar vancosamine, two  $\beta$ -hydroxycholortyrosine units, and three oxygenated phenylglycine systems.<sup>57</sup> Vancomycin works by inhibiting the bacterial synthesis of peptidoglycan in the following manner.

The bacterial cell walls of *C. difficile* consists of peptidoglycan, which is composed of two polymers: N-acetylmuramic acid (NAM) and N-acetylglucosamine (NAG).<sup>57</sup> In the absence of vancomycin, peptide chains are able to form hydrogen bonds with the NAM and NAG backbone, and the enzyme transpeptidase is able to cross-link the peptide chains, allowing for the synthesis of peptidoglycan. The site of this bond is the d-alanyl d-alanine residue at the end of the peptide chain. When vancomycin is introduced, it binds to that d-alanyl d-alanine residue, preventing transpeptidase from completing the cross-linkage, and peptidoglycan subsequently does not form, causing the cell wall to disintegrate.<sup>58</sup>

### 2.5.2 Advantages and Disadvantages of Vancomycin

According to Bartlett, metronidazole has sometimes been favored, due to its low cost, lower disposition for abuse, and possible decrease in likelihood for vancomycin-



resistant enterococci.<sup>59</sup> On the contrary, vancomycin has numerous advantages including its long history of use, key pharmacological characteristics (especially for an intra-luminal pathogen), and lack of apparent, adverse side effects. Through *in vitro* clinical trials of both drugs, results have indicated a consistent activity against CDI, and, in both cases, there has been no convincing evidence of drug resistance. Rate of relapse for both drugs is estimated to occur in about 15 to 25 percent of cases.<sup>54</sup>

It is believed that the distinguishing factor between the effectiveness of the two drugs is the degree of absorptivity along the path to the target area of the colon. Since metronidazole is completely absorbed in the small bowel, low levels of the antibiotic to reach the colonic lumen, which ultimately fails to prevent the production of colitis-causing toxins. Conversely, vancomycin is better able to resist absorption along its path to the colon, thus allowing for higher concentrations of the drug to reach its target area and effectively prevent the production of colitis-causing toxins.<sup>43</sup> A recent study conducted by the University of Illinois at Chicago further provides supporting evidence that vancomycin is a more effective treatment than metronidazole in those patients who are judged to have a severe form of the disease. Results of the study show clear superiority for vancomycin in terms of cure rates for those with severe symptoms (76% vs. 97%; P=.02).<sup>60</sup> Metronidazole and vancomycin have similar risks of recurrence, but vancomycin has resulted in fewer deaths.<sup>61</sup> The conclusion of this study ultimately indicated that vancomycin is the preferred drug for the treatment of seriously ill CDI patients since it comparatively maintains superior efficacy over other treatment options.<sup>57</sup> Furthermore, a 2017 study confirmed this fact, demonstrating a statistically significant reduction in all-cause 30-day mortality from severe CDI treated with vancomycin compared to metronidazole. Therefore, it can be

concluded that, while metronidazole may be effective in treating mild to moderate cases, vancomycin should be reserved for more effective treatment of severe cases of infection.<sup>48</sup>

### **2.5.3 Recolonization after Antibiotic Treatment**

A major precursor for *C. difficile* infection is the use of antibiotics. After a course of antibiotics, the normal gut flora will be depleted, and there is a chance that the microbiome of the GI tract will be recolonized by different bacteria than those that existed previously. Another study found that after broad spectrum antibiotic treatment, bacteria from the phylum *Verrucomicrobia*, specifically *A. muciniphila*, recolonized the digestive tract at a concentration of over 40 percent.<sup>62</sup> Concentrations this high had never been previously reported, and earlier analysis showed that *A. muciniphila* constituted no more than 1% of fecal cells.<sup>63</sup> Recently, FMT has emerged as a potential treatment for *C. difficile*. In a fecal transplant, the feces of healthy individual is administered via nasogastric and nasoduodenal tubes, a colonoscope, or as a retention enema.<sup>64</sup> This reintroduces the normal flora to the gut, allowing normal bowel function to resume.<sup>65</sup> Although the procedure has seen limited use, the published results from 100 patients treated with FMT show a 90% cure rate.<sup>65</sup> This process of recolonization will be analyzed with a drug whose usefulness is well known first in order to assess the efficacy of the gut-on-a-chip model, and later move on to applications with new and experimental drugs, including but not limited to FMT.

## **Chapter 3: Methodology**

### **3.1 Objectives**

This chapter will focus on the fabrication of the gut-on-a-chip device, in addition to the fabrication, integration and calibration of the glucose sensor that is integrated into the model. The gut-on-a-chip is a two-channel microfluidic device, which is created using soft lithography. This is the ideal method due to its flexible applicability to different materials and ability to facilitate the modeling of the surface chemistry of the gut. The sensor design incorporates a catechol chitosan redox capacitor and gold electrode, and enables monitoring of glucose concentration changes in the presence of bacteria and/or antibiotic. It is shown that the sensors developed have potential to accurately model the biochemical changes in the gut during infection and drug administration. As noted above, the methodology we have developed for the incorporation of an enzyme-based redox biosensor is completely new. It takes advantage of the unique pH-dependent solubility of chitosan and the redox-actuated ability to covalently incorporate glucose oxidase.

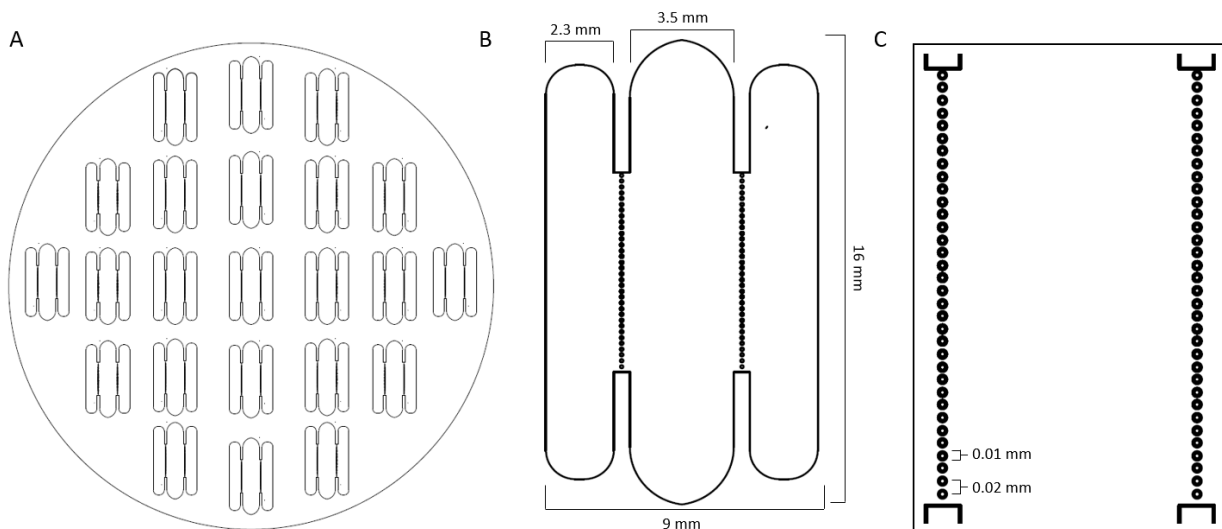
### **3.2 The Gut-On-A-Chip**

#### **3.2.1 Chip Component Design**

Two gut-on-a-chip models are designed. The first design is an “X” shape that has a 0.2 mm wide central channel and 1 mm wide arms (Figure 4.1A). The overall dimensions of this chip are 8 mm by 5.5 mm. This design is created with the intention of 3D printing of microvilli within the central channel. Conversely, the second design integrates the pores into the structure of the chip. This version of the chip optimizes the increased surface area for cell growth and proliferation. The dimensions of the chip are approximately 16 mm by

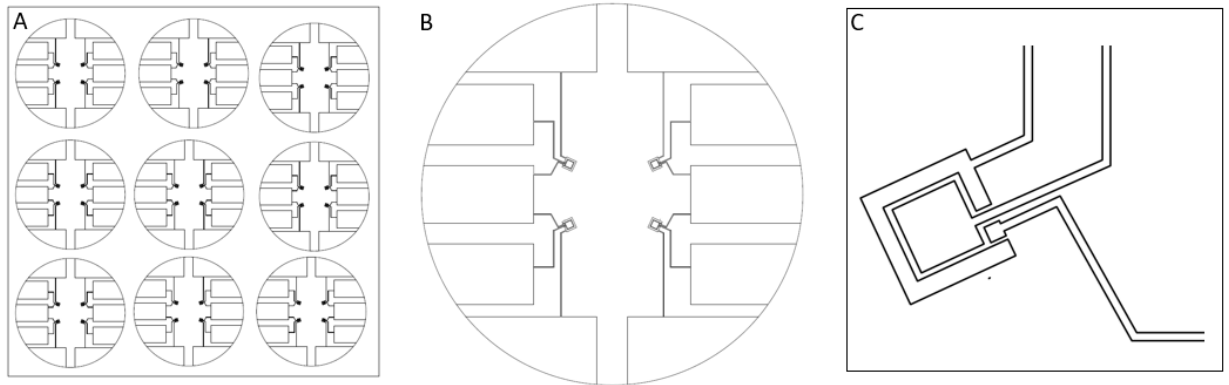
9.15 mm with the outer two channels being 2.3 mm in thickness and the central channel being 3.5 mm in thickness (Scheme 3.1B). The pillars between the channels have a diameter of 0.01 mm and are 0.02 mm apart (Scheme 3.1C).

Prior to chip fabrication, the designs are drawn on Autodesk Inventor and viewed in autoCAD, which are both computer aided design softwares. This designs are printed on plastic film by CAD/Art Services, Inc.



**Scheme 3.1** (A) The photomask designed using AutoCAD software depicting the multiple chip copies per silicon wafer (B) The 3-section chip designed using AutoCAD software. (C) AutoCAD design of the pillars aligned between the channels.

The design for the gold electrode stencil (Scheme 3.2) is also drawn on Autodesk Inventor. The three-electrode system consists of the outer counter electrode, the square shaped working electrode and the small reference electrode. The design is spaced so that the electrode is centered at the ends of the outer channels. This 302/304 stainless steel full hard stencil is made by Thin Metal Parts<sup>©</sup> (Colorado Springs, CO).



**Scheme 3.2** (A) The design of the gold electrode stencil (B) One of the gold electrode designs, 30 mm in diameter, with four three-electrode systems. (C) Three-electrode system design

The three separate sections shown in Scheme 3.1B fit cells in the center section and the 3-electrode sensor system in the outer sections. A line of pillars, signified by the dots between channels in Scheme 3.1C, allow for the flow of media over the electrodes whilst keeping the Caco-2 cells confined to the center compartment so as not to interfere with the sensor function. The masks obtained from CAD/Art Services Inc. and Thin Metal Parts are used to create a silicon wafer, which is then used to create the final PDMS chip with gold electrodes, as explained in Sections 3.2.2 and 3.2.3.

### 3.2.2 Fabrication of the Chip

The mask shown in Scheme 3.1 is used to create an SU-8 photoresist mold using standard soft lithography methods. A 4-in. silicon wafer is sterilized with acetone, isopropanol (IPA), and distilled water before 5 mL of SU-8 2050 photoresist (MicroChem, Westborough, MA) is deposited on the wafer, which is then spun at 2600 rpm for 30 seconds and baked in a pre-exposure phase at 95°C for 15 minutes. The design is imprinted onto the SU-8 mold through UV light exposure (405 nm wavelength) at 23.4 mW·cm<sup>-2</sup> using an EVG 620 mask aligner (Electronic Visions Inc., Phoenix, AZ). The wafer undergoes a post-exposure baking phase at 95°C for another 15 minutes before being agitated in a solution of SU-8 developer (MicroChem, Westborough, MA) for 10 minutes.

Residual SU-8 is rinsed away by isopropanol and deionized (DI) water. The final SU-8 mold is then left to air-dry and can be reused.

An elastomeric block of polydimethylsiloxane (PDMS) (Sylgard 184, Dow Corning Co., Midland, MI) is fashioned using the SU-8 photoresist mold. The PDMS and curing agent is mixed at a ratio of 10:1, respectively, and baked at 65°C for approximately 1 hour. Once solidified, the PDMS is delaminated from the mold. Finally, a 1.0 mm Harris Uni-Core™ (Ted Pella, Inc., Redding, CA) biopsy punch is used to punch inlet and outlet holes in the PDMS design. In order to complete the gut-on-a-chip model, this PDMS base must be plasma bonded to a glass coverslip containing the gold electrode sensor with the appropriate design.

### **3.2.3 Fabrication of the Gold Electrode**

To create the gold electrode pattern on the glass cover slide, the cover slide is carefully aligned and attached to the mask. The chamber of the METRA Vacuum Equipment Machine is isolated by turning off the gauge and closing the gate valve, and filled with nitrogen through the rotation of the turbo molecular pump. The gold boat and chrome rod are clamped into the electrodes, before the mask can be secured into place above the shutter. The air is pulled out of the chamber to decrease the pressure reading to 150 mTorr. The ionization gauge is then turned on to form the current on the rear electrode before the control setting is switched back to the front electrode. The density for the chrome is set to  $7.200 \text{ g}\cdot\text{cm}^{-3}$  with a Z-ratio of 0.305. 100 A of current are outputted to lower the pressure, after which the output control is gradually increased from  $1 \text{ A}\cdot\text{s}^{-1}$  to  $50 \text{ A}\cdot\text{s}^{-1}$  to deposit the chrome adhesive layer. Before depositing the gold, the shutter and power supply are turned off to again increase the pressure. From the rear electrode, the output control is

slightly increased and the density is changed to  $19.3 \text{ g}\cdot\text{cm}^{-3}$ , with a Z-ratio of 0.381 for the gold deposition. When the rate of deposition reaches its maximum and the thickness of the gold reaches approximately 1 mm, all power supply and valves are turned off before removing the mask from the chamber. The gold deposited cover slides are then ready for oxygen plasma treatment (IPC 4000 series plasma system) (Branson, PA). The PDMS chip and gold electrode cover slide are aligned appropriately and plasma bonded to form a single microfluidic device.

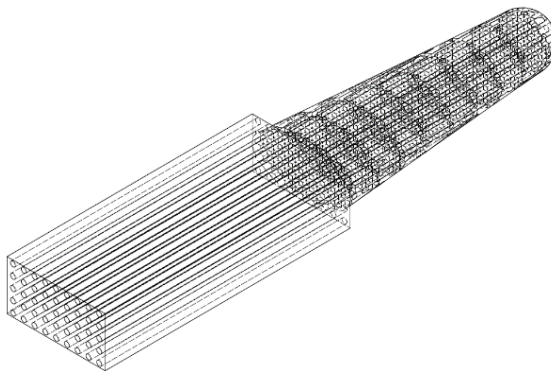
### **3.2.4 Three-Dimensional Printing Microvilli**

Using Autodesk Inventor CAD software, a single microvillus with the following dimensions is tailored: 0.2 mm wide and 1 mm long. The vertical pores at the base and circular pores at the tip are  $10 \mu\text{m}$  in diameter (Scheme 3.3). These characteristics mimic the finger-like shape and projection of intestinal microvilli. This design is uploaded to the DeScribe software, which is compatible with the NanoScribe Photonic Professional GT 3D printer (Nanoscribe, Eggenstein).

A top-down printing method, adapted from the methodology of Bioengineering PhD candidate, Wu Shang, is used to 3D print porous microvilli directly into the sol gel-coated central channel of the “X” shaped chip. Using the DeScribe software, the initial laser power is set to 80%, and decreased by increasing increments with each layer to prevent the possibility of burning.

To prepare the substrate for printing, a circular glass coverslip is first washed with acetone, IPA, and water, and dried completely. The coverslip is then secured in a perforated holder. A drop of oil is placed on the back side of the coverslip and OrmoComp is placed on the front side for printing. The entire holder is then placed under the 63X objective lens

of the printer, and the “inverted z-axis” setting is selected to print using a top-down approach. The completed print can then be imaged using a microscope.



**Scheme 3.3** CAD drawing of porous microvilli

### **3.3 Cell Studies**

#### **3.3.1 Preliminary Caco-2 Cell Culture**

Human intestinal epithelial Caco-2 cells (Caco-2 BBE human colorectal carcinoma cells) are grown in Dulbecco’s Modified Eagle Medium (DMEM, Gibco, Grand Island, NY) containing  $4.5 \text{ g}\cdot\text{L}^{-1}$  glucose,  $100 \text{ units}\cdot\text{mL}^{-1}$  penicillin, and  $100 \text{ mg}\cdot\text{mL}^{-1}$  streptomycin (Gibco), 25 mM HEPES supplemented with 10% fetal bovine serum (FBS). These cells are maintained at  $37^{\circ}\text{C}$  in a humidified incubator under 5%  $\text{CO}_2$ . Cells are maintained according to ATCC standards.<sup>63</sup> The cells are grown to 75% confluency before seeding inside the device.

#### **3.3.2 Implantation of Caco-2 cells into gut-on-a-chip model**

The microfluidic device is first sterilized by injecting 70% (v/v) ethanol into the microchannels and dried in an oven heated to  $65^{\circ}\text{C}$  for 10 minutes. Then, the device is exposed to UV light for 40 minutes. The channels are coated with type I collagen and matrigel mixture for the next 2 hours. Caco-2 cells are inserted into the device at a



confluency of  $1.5 \times 10^5$  cells $\cdot$ cm $^{-2}$  and allowed to settle for 1 hour. DMEM is continuously flowed at a rate of 30  $\mu$ L $\cdot$ h $^{-1}$  using a Genie<sup>TM</sup> Plus Syringe Pump (Kent Scientific, Torrington, CT) and replenished when needed.

### **3.4. The Sensors**

#### **3.4.1 Electrodeposition Solution Preparation**

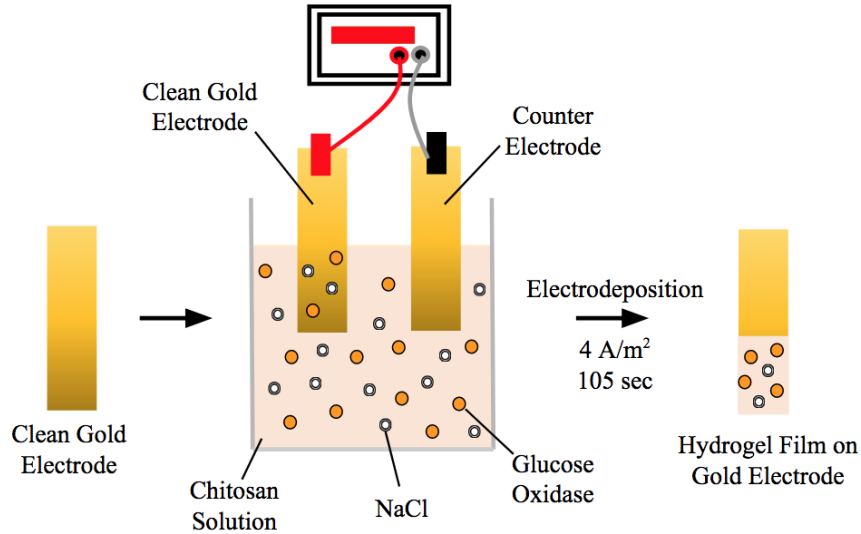
In this phase, a chitosan solution with GOx is created for subsequent electrodeposition. First, a 1% (w/w) chitosan solution is prepared by dissolving chitosan flakes in an acidic solution.<sup>47</sup> The acidic solution consists of acetic acid (HAc) and deionized water. After two hours, if the pH is between 5 and 6, but the chitosan flakes are not dissolved, HAc is added dropwise until the chitosan is fully dissolved. If the pH is below 4, more chitosan flakes are added. The solution is finally filtered to remove any remaining undissolved particles.

Next, the anodic electrodeposition solution is created by adding GOx and sodium chloride (NaCl) to the previously prepared chitosan. The previously made chitosan solution is combined with GOx (680 U $\cdot$ mL $^{-1}$ ) and NaCl (0.15 M).<sup>47</sup>

#### **3.4.2 Electrodeposition**

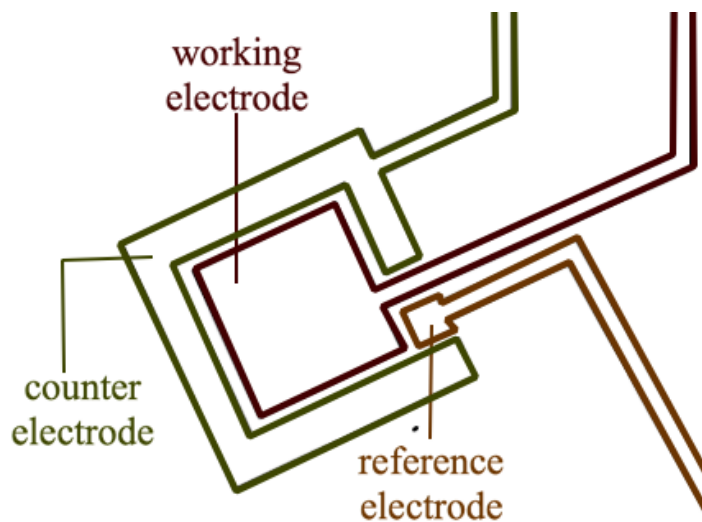
This phase focuses on glucose sensor fabrication. First, a preliminary sensor is created on an external gold electrode in order to perfect protocol design and testing methods. The base of the sensor is a two-dimensional silicon wafer, on which a layer of gold is deposited. The circular wafer is cut into rectangular pieces, where each piece will become a single sensor.

Next, a gold electrode and counter electrode are immersed in the electrodeposition solution. The electrodes are connected to a potentiostat. For anodic deposition, the anode is the working electrode and the cathode is the counter electrode.<sup>47</sup> A current density of  $4 \text{ A}\cdot\text{m}^{-2}$  is applied for 105 seconds. After electrodeposition, the electrode is rinsed carefully with water.



**Scheme 3.4** *Electrodeposition set-up on external electrode*

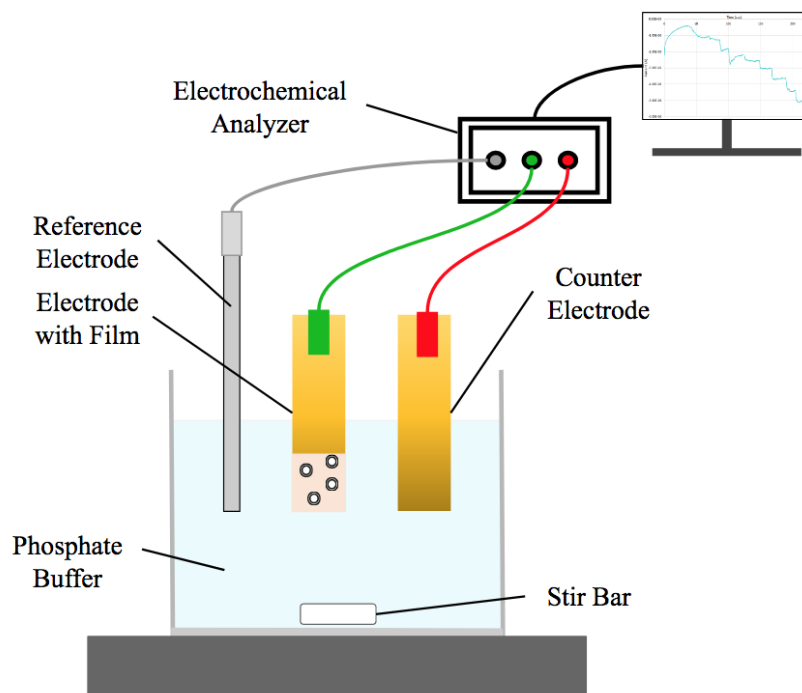
The electrodeposition methodology is then adapted to create a sensor for use in the microfluidic device. Gold is deposited on a glass cover slide and plasma bonded with the microfluidic device to create the gold electrode (Section 3.2.3). A three-electrode system is utilized for electrodeposition and testing (Scheme 3.5). Using a syringe, the channel is completely filled with the electrodeposition solution. The counter and working electrodes are connected to the potentiostat and a current density of  $4 \text{ A}\cdot\text{m}^{-2}$  is applied for 105 seconds. After electrodeposition, a 0.15 M phosphate buffer solution is flowed through the channel to rinse the electrodes.



**Scheme 3.5** *The 3-electrode system utilized for deposition and testing of the glucose sensor. Deposition requires a counter and working electrode. Sensor testing requires the additional reference electrode. There are four electrode systems spaced throughout the device.*

### 3.4.3 Sensor Testing

20% glucose is mixed with 0.15 M phosphate buffer to create the following concentration solutions: 2 mM, 4 mM, and 6 mM. In order to test the preliminary sensor, the working, counter, and reference electrodes are connected to the CHI6273C Electrochemical Analyzer (CH. Instruments, Inc., Austin, TX). The electrodes are submerged in the different concentrations of glucose solution sequentially and a constant voltage of 0.6 V is applied. The resulting current is measured and graphs for each glucose concentrations are obtained. The same process is used to test the integrated sensor; however, the glucose solutions are flowed through the channel instead of submerging the sensors in a beaker.



**Scheme 3.6.** *External sensor testing set-up*

## Chapter 4: Results

### 4.1 Creation of the Gut Microenvironment

It was hypothesized that creating a PDMS gut-on-a-chip model with 3D printed microvilli structures will mimic the absorption and passage of nutrients and wastes from the human gut epithelial cells to the surrounding environment. The initial gut-on-a-chip design was fabricated with an “X” shaped design where Caco-2 cells were concentrated in the center and the media was contained at the ends of the design (Figure 4.1A). This design was optimal for microvilli incorporation in the center of the “X.” A single microvillus structure, 200  $\mu\text{m}$  high and 60  $\mu\text{m}$  wide, was 3D printed using the Nanoscribe printer and visualized using confocal microscopy (Figure 4.1B and C). The lack of contrast in Figure 4.1B indicates an unstable print, and the wavy demarcations between the vertical and circular pores of the villus in Figure 4.1C demonstrate low resolution.

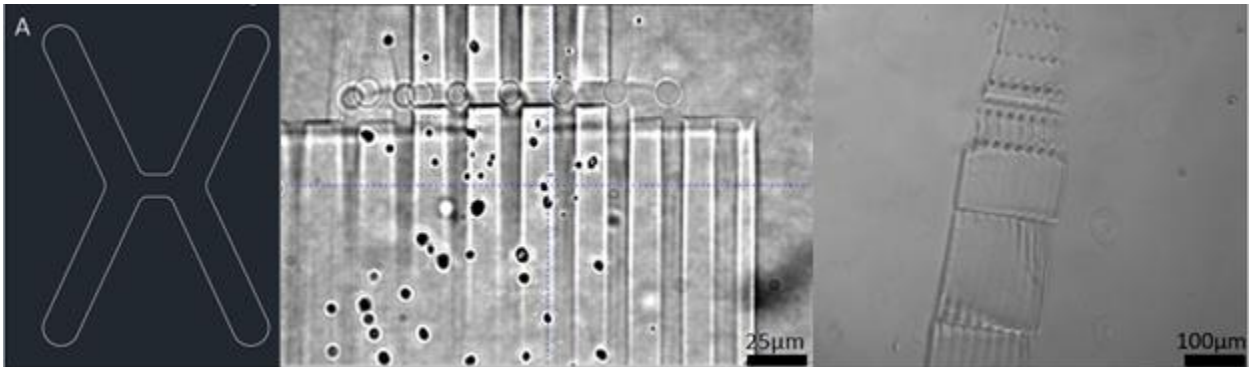


**Figure 4.1** (A) Initial design of the PDMS gut-on-a-chip design in an “X” design. The width of the central channel is 0.2 mm wide. (B) 40X image of print with minimal spotted burning and (C) 20X confocal microscopy images of 3D printed porous microvilli outside of the gut-on-a-chip, using the NanoScribe 3D printer.

Due to limitations in the 3D printer, an alternative design that replaced the need for microvilli was fashioned and tested. It was hypothesized that an alternative design of the gut-on-a-chip model with a larger middle channel separated by PDMS pillars to prevent the infiltration of the cells into the other channels and still allow for the diffusion of

nutrients and wastes would be superior. The larger middle channel held Caco-2 cells, and the two outer channels contained media to provide nutrients to, collect waste from, and maintain viability of the Caco-2 cells. To test this hypothesis, the cells seeded inside the PDMS gut-on-a-chip model were imaged using confocal microscopy immediately after seeding and after 1 day of incubation (Fig. 4.2A and B). The cells increased in both number and size 24 hours after seeding within the chip, forming a monolayer.

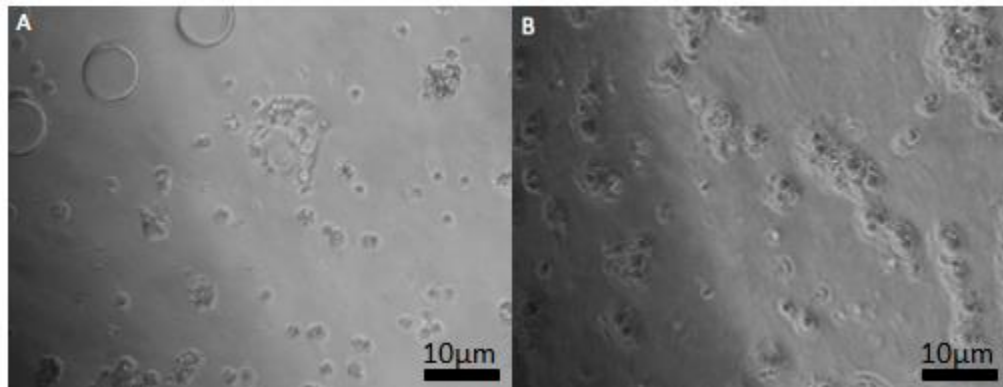


**Figure 4.2** (A) Cells seeded in the chip and aggregated around the PDMS pillars at 0H. (B) Cells, viewed at 10X under confocal microscopy, adhered to the chip at 24H post-seeding.

## 4.2 Integration of Gold Electrode Sensors

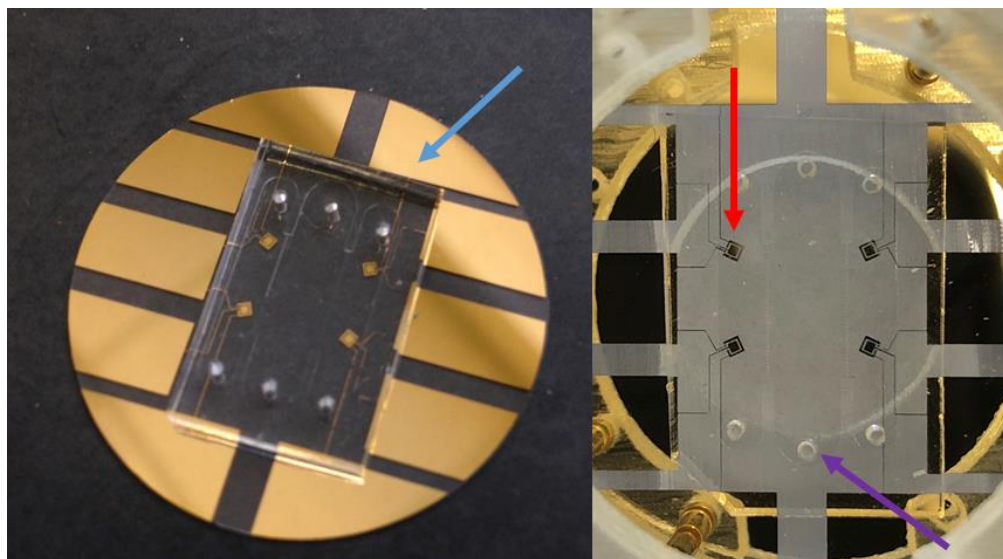


**Figure 4.3** The final PDMS gut-on-a-chip model plasma bonded to the glass slide with gold electrodes. The blue arrow indicates one of the ten contact electrodes around the chip for easy access to connect to a current source. The red arrow indicates one of the four sensor systems on the outer channels of the chip. The purple arrow indicates one of six total inlet holes.

It was hypothesized that the inclusion of glucose oxidase in the catechol-chitosan redox sensor would allow for the measurement of the glucose concentration in a sample.<sup>47</sup> The glucose sensor was created on one of the three-electrode systems in the model as shown in Figure 4.3. Amperometric I-t experiments to test sensor functionality were conducted using glucose concentrations of 2 mM, 4 mM, and 6 mM. When glucose solutions were added to the chip model, an immediate current response was induced as shown in Figure 4.4. The current response was linearly proportional to the concentration of glucose in the solution; larger concentrations of glucose resulted in a larger current. Using the current responses for sequential concentrations, a standard curve was created by plotting current versus glucose concentration. As shown in Figure 4.5, an  $R^2$  value of 0.9223 was obtained for one such sensor.

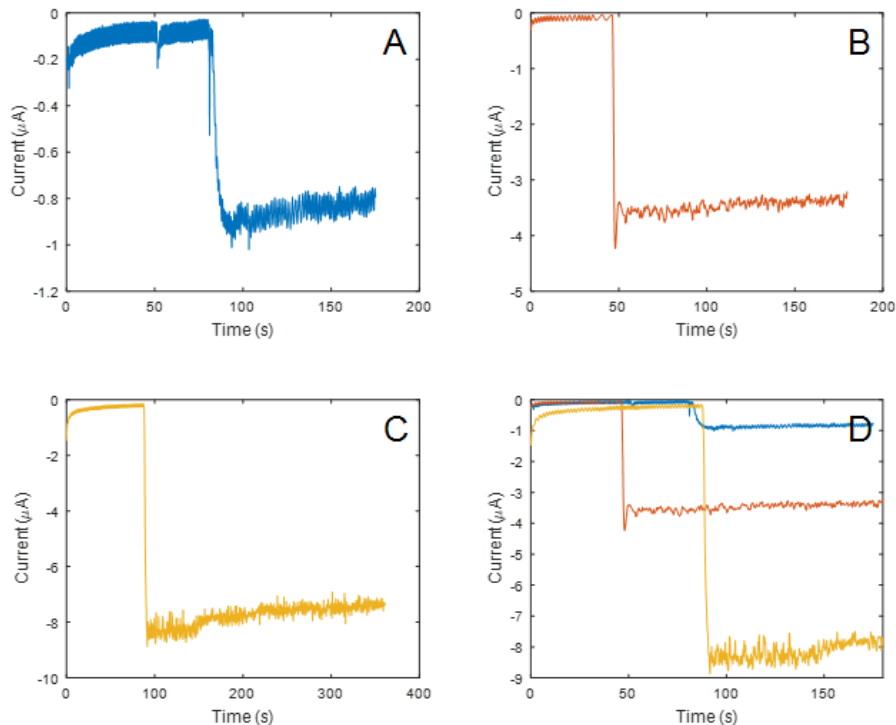


**Figure 4.4** Current response of glucose sensor upon addition of 2 mM (A), 4 mM (B), and 6 mM (C) glucose solutions. The sharp decline in current indicates the addition of the glucose solution. Graphs A, B and C are compiled into one graph (D).

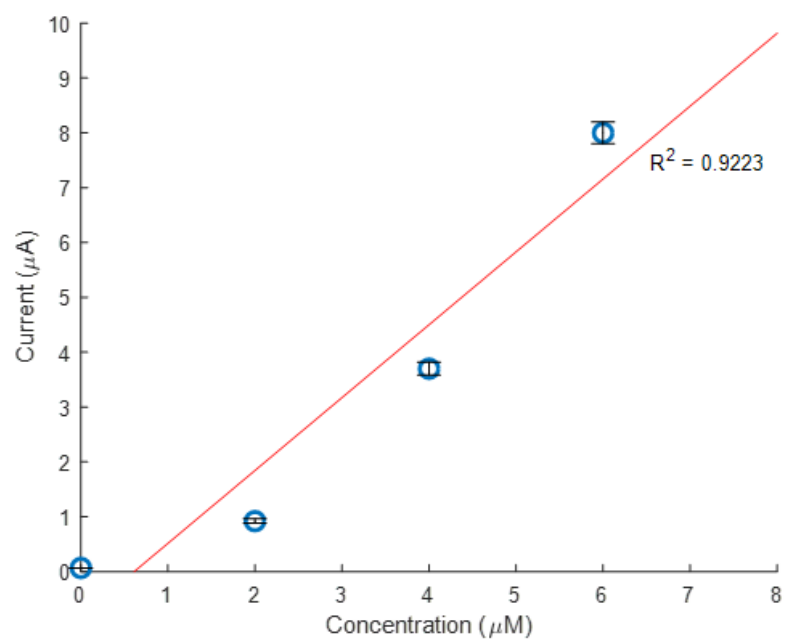


**Figure 4.5** Standard curve of current versus glucose concentration created using sensor output data from separate glucose concentrations.  $R^2 = 0.9223$ .



## Chapter 5: Discussion

These findings suggest that (i) PDMS gut-on-a-chip models can mimic the human gut's ability to passage nutrients and wastes from Caco-2 cells to the environment, and (ii) gold electrode sensors deposited in the model are able to detect glucose.

### 5.1 3D Printing of the Microvilli Structures

The gut-on-a-chip model can serve as an alternative *in vitro* model to mimic the human gut and test novel drug treatments. One of the original objectives of this research was to improve the structural accuracy of the existing gut-on-a-chip model. In order to achieve this, microvilli structures were created to increase absorption. In this study, these microvilli structures were 3D printed into the gut-on-a-chip model (Figure 4.1) with an initial prototype design. Initial 3D printing attempts resulted in burning, which, due to the high laser power, was inferred. The laser power was experimentally reduced in various increments to determine the optimal settings that would produce a stable print implanted in the substrate without burning. However, it was discovered that the degree of burning was arbitrary and the most favorable laser power for each layer of the print could not be determined.

The least amount of burning was seen in the print where the initial laser power was set to below 80% and decreased incrementally with each layer (Figure 4.1B). Unfortunately, decreased laser power seemed to excessively compromise the stability of the microvillus in the substrate (Figure 4.1C). Two factors may have contributed to this “floating” print. First, a tiny crack in the coverslip, which seemed to be out of the vicinity of the print, may have increased under the laser beam. Second, even with an intact

coverslip, overall inconsistency and lack of correlation between laser power adjustment and amount of burning suggests a possible limitation of the 3D printer.

Burning seemed to occur most frequently at the interface of the vertically porous and circularly porous parts of the villus, which indicates that the printer may be unable to effectively resolve the sudden structural change. This discovery warrants a project of its own dedicated to testing different iterations of a porous design, ranging from a simple block to structures closely resembling actual microvilli. Because 3D printing of microvilli was deemed overly ambitious and infeasible within the available time constraints, a new chip design with an integrated filtration system was developed. To further improve the accuracy of the gut-on-a-chip model, future research may be focused on refining 3D printing to successfully incorporate porous microvilli. To increase the superiority of this gut-on-a-chip model, a new design was proposed.

## **5.2 Biofabrication of an alternative PDMS gut-on-a-chip model**

This PDMS chip served its purpose as a biocompatible device in which to seed cells, as shown in Figure 4.2. The current 3-channel design would enable maximum cell seeding and optimal sensor readings since cells are restricted to the middle channel, while fluid flow throughout all three channels allows for data collection by sensors. Although the pillars did not successfully keep all of the cells out of the two outer channels during initial seeding (Figure 4.2A), they prevented excessive migration and growth on the sensors. During the seeding period, cell viability was monitored by qualitatively analyzing cell confluency and size. Due to the microscopic surface area for cells to grow in, the cells were observed after a period of only one day to determine cell viability. The formation of

monolayer after cell seeding is a good indication that the cells had adapted to the growth conditions in the chip and begun to mimic the endothelial cell growth formations in the gut. However, medium evaporation depleted the cells of nutrients to maintain viability within the device.

Medium evaporation became an unexpected challenge with cell culture in which there are several plausible explanations for this phenomenon. There may be too many inlets and outlets, allowing for culture medium to easily escape the device. The humidity of the device also may not have been properly maintained, causing the device to dehydrate. Additional experiments and trials are needed to eliminate this issue. Humidity can be restored and maintained by saturating the local environment with distilled water or PBS solution. Furthermore, future device designs may also limit the number of inlets and outlets or adequate inlet and outlet plugs can reduce evaporation.

### **5.3 Integration of gold electrode sensors**

Functional catechol-chitosan redox sensors with glucose oxidase can be created within the gut-on-a-chip model to measure glucose concentration levels in a sample. The graphs depicting the current response (Figure 4.4) have some noise before and after the addition of glucose that is caused by the movement of the stir bar in the beaker. Nonetheless, stirring was crucial to ensure that the glucose was evenly distributed throughout the water. Despite the noise, the sensor output of known glucose concentrations led to the creation of a standard curve for the sensor. This standard curve can be used to extrapolate glucose concentrations from unknown samples. Specific to this device, cell metabolism can be quantified. When exposed to a disease, quantifiable changes in cell metabolism can signify the effects of the disease on the intestinal microenvironment.

Consequently, potential novel treatments can be tested and effects can be quantified with the sensors to measure effectiveness.

The creation of the glucose sensor on external gold electrodes served as a proof-of-concept for the use of anodically-deposited catechol-chitosan redox sensors. Further testing must be conducted with the sensor deposited onto the gold electrodes within the chip model to ensure that the sensor fabrication methodology is effective. In the future, this sensor technology can be expanded to create a diverse range of sensors so long as a redox molecule, such as  $H_2O_2$ , is created during the reaction.

## Chapter 6: Conclusion

This research demonstrated the ability to improve existing microfluidic models of the GI tract through the assembly and electrodeposition of a glucose sensor into a gut-on-a-chip device. Results from sensor testing showed that glucose concentration can be monitored at specific sites in the microfluidic device in real-time. Furthermore, preliminary cell studies indicated that cells could be seeded into a gut-on-a-chip device, and identified medium evaporation as a challenge to cell proliferation and viability for future works. Attempts at 3D-printing microvilli into the initial gut-on-a-chip design revealed challenges associated with directly printing into a PDMS base, such as arbitrary burning. Overall, these results provide a foundation for future research involving improving the accuracy of the gut-on-a-chip model by showing the feasibility of monitoring changing environmental conditions in the GI tract *in vivo* during pharmaceutical testing.

In terms The original intention of utilizing the OoC device for the purpose of testing vancomycin on *C. difficile* remains of high priority. The vast array of research supporting the effectiveness of vancomycin in the treatment of *C. difficile* suggests that this long-standing disease and treatment model would lend great support in testing the OoC and illustrating the effectiveness of the device by providing a platform to obtain more detailed and comprehensive data at a level previously unavailable.

The ultimate ambition of this research remains to expedite drug testing and make the process more efficient and effective than the current FDA standard review process. This device has the potential beacon to eliminate human and animal testing by supporting and upholding drug evaluation to a superior standard than that which currently exists. The incorporation of sensors in the OoC device can increase functionality of not only gut on a

chip models, but in all available types of OoC's. Structural improvements, combined with successful integration of sensors, creates the potential for a more efficient and perhaps a faster drug screening process, which will ultimately benefit pharmaceutical and biomedical research companies as well as the general public. It is in the best interest of these stakeholders that research on OoC models continues to progress so that the research community may continue to combat current limitations in traditional drug testing and maintain the utmost confidence in efficiently testing drugs without animal or human test subjects.

## References

1. About tissue chip. National Center for Advancing Translational Sciences. <http://www.ncats.nih.gov/tissuechip/about>. Accessed September 20, 2015.
2. Research C for DE and. Special features - Frequently asked questions about the FDA drug approval process. <http://www.fda.gov/Drugs/ResourcesForYou/SpecialFeatures/ucm279676.htm>. Accessed September 29, 2015.
3. Ghaemmaghami AM, Hancock MJ, Harrington H, Kaji H, Khademhosseini A. Biomimetic tissues on a chip for drug discovery. *Drug Discov Today*. 2012;17(3-4):173-181. doi:10.1016/j.drudis.2011.10.029
4. Wu M-H, Huang S-B, Lee G-B. Microfluidic cell culture systems for drug research. *Lab Chip*. 2010;10(8):939-956. doi:10.1039/B921695B
5. Jong M de, Maina T. Of mice and humans: Are they the same?—Implications in cancer translational research. *J Nucl Med*. 2010;51(4):501-504. doi:10.2967/jnumed.109.065706
6. Guillouzo A, Guguen-Guillouzo C. Evolving concepts in liver tissue modeling and implications for in vitro toxicology. *Expert Opin Drug Metab Toxicol*. 2008;4(10):1279-1294. doi:10.1517/17425255.4.10.1279
7. Colon cancer treatment. National Cancer Institute. <http://www.cancer.gov/types/colorectal/patient/colon-treatment-pdq>. Accessed November 28, 2015.
8. Gastrointestinal tract - National library of medicine. PubMed Health. <http://www.ncbi.nlm.nih.gov/pubmedhealth/PMHT0022855/>. Accessed September 20, 2015.
9. McDowell J. Small intestine. In: *Encyclopedia of Human Body Systems*. ABC-CLIO; 2010.
10. The large intestine: MedlinePlus Medical Encyclopedia Image. <https://www.nlm.nih.gov/medlineplus/ency/imagepages/8832.htm>. Accessed December 5, 2015.
11. Esch EW, Bahinski A, Huh D. Organs-on-chips at the frontiers of drug discovery. *Nat Rev Drug Discov*. 2015;14(4):248-260. doi:10.1038/nrd4539
12. Kim HJ, Huh D, Hamilton G, Ingber DE. Human gut-on-a-chip inhabited by microbial flora that experiences intestinal peristalsis-like motions and flow. *Lab Chip*. 2012;12(12):2165. doi:10.1039/c2lc40074j

13. Kim J, Lee H, Selimović Š, Gauvin R, Bae H. Organ-on-a-chip: Development and clinical prospects toward toxicity assessment with an emphasis on bone marrow. *Drug Saf.* 2015;38(5):409-418. doi:10.1007/s40264-015-0284-x
14. Gamboa JM, Leong KW. In vitro and in vivo models for the study of oral delivery of nanoparticles. *Adv Drug Deliv Rev.* 2013;65(6):800-810. doi:10.1016/j.addr.2013.01.003
15. Kim HJ, Ingber DE. Gut-on-a-Chip microenvironment induces human intestinal cells to undergo villus differentiation. *Integr Biol.* 2013;5(9):1130-1140. doi:10.1039/C3IB40126J
16. Hoffman RM. The three-dimensional question: can clinically relevant tumor drug resistance be measured in vitro? *Cancer Metastasis Rev.* 1994;13(2):169-173.
17. Neuži P, Giselbrecht S, Länge K, Huang TJ, Manz A. Revisiting lab-on-a-chip technology for drug discovery. *Nat Rev Drug Discov.* 2012;11(8):620-632. doi:10.1038/nrd3799
18. Bhatia SN, Ingber DE. Microfluidic organs-on-chips. *Nat Biotechnol.* 2014;32(8):760-772. doi:10.1038/nbt.2989
19. Zhou J, Niklason LE. Microfluidic artificial “vessels” for dynamic mechanical stimulation of mesenchymal stem cells. *Integr Biol.* 2012;4(12):1487-1497. doi:10.1039/C2IB00171C
20. Yu J, Peng S, Luo D, March JC. In vitro 3D human small intestinal villous model for drug permeability determination. *Biotechnol Bioeng.* 2012;109(9):2173-2178. doi:10.1002/bit.24518
21. Ren K, Zhou J, Wu H. Materials for microfluidic chip fabrication. *Acc Chem Res.* 2013;46(11):2396-2406. doi:10.1021/ar300314s
22. Weltin A, Slotwinski K, Kieninger J, et al. Cell culture monitoring for drug screening and cancer research: a transparent, microfluidic, multi-sensor microsystem. *Lab Chip.* 2013;14(1):138-146. doi:10.1039/C3LC50759A
23. Luo X, Tsao C-Y, Wu H-C, et al. Distal modulation of bacterial cell-cell signalling in a synthetic ecosystem using partitioned microfluidics. *Lab Chip.* 2015;15(8):1842-1851. doi:10.1039/c5lc00107b
24. Xia Y, Whitesides GM. Soft lithography. *Annu Rev Mater Sci.* 1998;28(1):153-184. doi:10.1146/annurev.matsci.28.1.153
25. Unger MA. Monolithic microfabricated valves and pumps by multilayer soft lithography. *Science.* 2000;288(5463):113-116. doi:10.1126/science.288.5463.113



26. Kim E, Xiong Y, Cheng Y, et al. Chitosan to connect biology to electronics: fabricating the bio-device interface and communicating across this interface. *Polymers*. 2014;7(1):1-46. doi:10.3390/polym7010001
27. E. A. Johannessen LW. Implementation of multichannel sensors for remote biomedical measurements in a microsystems format. *Biomed Eng IEEE Trans On*. 2004;51(3):525-535. doi:10.1109/TBME.2003.820370
28. Wittkamp M, Chemnitiu G-C, Cammann K, Rospert M, Mokwa W. Silicon thin film sensor for measurement of dissolved oxygen. *Sens Actuators B Chem*. 1997;43(1-3):40-44. doi:10.1016/S0925-4005(97)00138-X
29. Abramova N, Ipatov A, Levichev S, Bratov A. Integrated multi-sensor chip with photocured polymer membranes containing copolymerized plasticizer for direct pH, potassium, sodium and chloride ions determination in blood serum. *Talanta*. 2009;79(4):984-989. doi:10.1016/j.talanta.2009.03.023
30. Sambuy Y, Angelis ID, Ranaldi G, Scarino ML, Stammati A, Zucco F. The Caco-2 cell line as a model of the intestinal barrier: influence of cell and culture-related factors on Caco-2 cell functional characteristics. *Cell Biology and Toxicology*. 2005;21(1):1-26. doi:10.1007/s10565-005-0085-6.
31. Williams SC, Patterson EK, Carty NL, Griswold JA, Hamood AN, Rumbaugh KP. *Pseudomonas aeruginosa* autoinducer enters and functions in mammalian cells. *J Bacteriol*. 2004;186(8):2281-2287.
32. Smith RS, Harris SG, Phipps R, Iglewski B. The *Pseudomonas aeruginosa* quorum-sensing molecule N-(3-oxododecanoyl)homoserine lactone contributes to virulence and induces inflammation in vivo. *J Bacteriol*. 2002;184(4):1132-1139.
33. Tateda K, Ishii Y, Horikawa M, et al. The *Pseudomonas aeruginosa* autoinducer N-3-oxododecanoyl homoserine lactone accelerates apoptosis in macrophages and neutrophils. *Infect Immun*. 2003;71(10):5785-5793.
34. Rackus DG, Dryden MDM, Lamanna J, et al. A digital microfluidic device with integrated nanostructured microelectrodes for electrochemical immunoassays. *Lab Chip*. 2015;15(18):3776-3784. doi:10.1039/C5LC00660K
35. Ghafar-Zadeh E, Sawan M. Capacitive sensing electrodes. In: *CMOS Capacitive Sensors for Lab-on-Chip Applications*. Analog Circuits and Signal Processing. Springer Netherlands; 2010:25-33. doi:10.1007/978-90-481-3727-5\_2
36. Bartlett JG. The case for vancomycin as the preferred drug for treatment of clostridium difficile Infection. *Clin Infect Dis*. 2008;46(10):1489-1492. doi:10.1086/587654
37. Morteau S, Chirt G, Beuran M. Clostridium difficile colitis in trauma patients - a global step by step review. *Maedica - J Clin Med*. 2015;10(2):163-169.

38. Taori SK, Wroe A, Hardie A, Gibb AP, Poxton IR. A prospective study of community-associated *Clostridium difficile* infections: The role of antibiotics and co-infections. *J Infect.* 2014;69(2):134-144. doi:10.1016/j.jinf.2014.04.002
39. Surmalyan A. Surface potential behavior in ISFET based bio-(chemical) sensors. *Armen J Phys.* 2012;5(4):194-202.
40. Wilcox MH, Fawley WN, Settle CD, Davidson A. Recurrence of symptoms in *Clostridium difficile* infection—relapse or reinfection? *J Hosp Infect.* 1998;38(2):93-100. doi:10.1016/S0195-6701(98)90062-7
41. Electrodeposition of Carbon Nanotubes Triggered by Cathodic and Anodic Reactions of Dispersants: Materials and Manufacturing Processes: Vol 30, No 6. <https://www.tandfonline.com/doi/abs/10.1080/10426914.2014.994771>. Accessed April 4, 2018.
42. Gray KM, Liba BD, Wang Y, et al. Electrodeposition of a Biopolymeric Hydrogel: Potential for One-Step Protein Electroaddressing. *Biomacromolecules.* 2012;13(4):1181-1189. doi:10.1021/bm3001155
43. Gerding DN, Muto CA, Owens RC. Treatment of *clostridium difficile* infection. *Clin Infect Dis.* 2008;46(Supplement 1):S32-S42. doi:10.1086/521860
44. Aslam S, Hamill RJ, Musher DM. Treatment of *clostridium difficile*-associated disease: old therapies and new strategies. *Lancet Infect Dis.* 2005;5(9):549-557. doi:10.1016/S1473-3099(05)70215-2
45. Surawicz CM, Brandt LJ, Binion DG, et al. Guidelines for diagnosis, treatment, and prevention of *Clostridium difficile* infections. *Am J Gastroenterol.* 2013;108(4):478-498; quiz 499. doi:10.1038/ajg.2013.4
46. Kaiser G. Peptidoglycan synthesis in a gram-positive bacterium. November 2014. <http://www.microbelibrary.org/library/bacteria/3661-peptidoglycan-synthesis-in-a-gram-positive-bacterium>. Accessed September 26, 2015.
47. Reynolds PE. Structure, biochemistry and mechanism of action of glycopeptide antibiotics. *Eur J Clin Microbiol Infect Dis.* 1989;8(11):943-950. doi:10.1007/BF01967563
48. Zar FA, Bakkanagari SR, Moorthi KMLST, Davis MB. A comparison of vancomycin and metronidazole for the treatment of *clostridium difficile*-associated diarrhea, stratified by disease severity. *Clin Infect Dis.* 2007;45(3):302-307. doi:10.1086/519265
49. Rohlke F, Stollman N. Fecal microbiota transplantation in relapsing *Clostridium difficile* infection. *Ther Adv Gastroenterol.* 2012;5(6):403-420. doi:10.1177/1756283X12453637

50. Stevens V, Nelson R, Khader K, et al. Recurrence and mortality following treatment for *Clostridium difficile* infection with metronidazole or vancomycin. *Antimicrob Resist Infect Control*. 2015;4(Suppl 1):O38. doi:10.1186/2047-2994-4-S1-O38
51. O'Connell M, Slish J, Shelly M. Efficacy of Oral Vancomycin, Oral Metronidazole, or IV Metronidazole Prophylaxis at Reducing the Risk of *Clostridium difficile* Recurrence. *Open Forum Infect Dis*. 2017;4(Suppl 1):S384. doi:10.1093/ofid/ofx163.952
52. Dubourg G, Lagier J-C, Armougom F, et al. High-level colonisation of the human gut by Verrucomicrobia following broad-spectrum antibiotic treatment. *Int J Antimicrob Agents*. 2013;41(2):149-155. doi:10.1016/j.ijantimicag.2012.10.012
53. Derrien M, Collado MC, Ben-Amor K, Salminen S, Vos WM de. The mucin degrader *Akkermansia muciniphila* Is an abundant resident of the human intestinal tract. *Appl Environ Microbiol*. 2008;74(5):1646-1648. doi:10.1128/AEM.01226-07
54. Bakken JS. Fecal bacteriotherapy for recurrent *Clostridium difficile* infection. *Anaerobe*. 2009;15(6):285-289. doi:10.1016/j.anaerobe.2009.09.007
55. Bakken JS, Borody T, Brandt LJ, et al. Treating *Clostridium difficile* infection with fecal microbiota transplantation. *Clin Gastroenterol Hepatol Off Clin Pract J Am Gastroenterol Assoc*. 2011;9(12):1044-1049. doi:10.1016/j.cgh.2011.08.014
56. Brandt LJ, Aroniadis OC, Mellow M, et al. Long-Term Follow-Up of Colonoscopic Fecal Microbiota Transplant for Recurrent *Clostridium difficile* Infection. *Am J Gastroenterol*. 2012;107(7):1079-1087. doi:10.1038/ajg.2012.60
57. Tan SH, Nguyen N-T, Chua YC, Kang TG. Oxygen plasma treatment for reducing hydrophobicity of a sealed polydimethylsiloxane microchannel. *Biomicrofluidics*. 2010;4(3). doi:10.1063/1.3466882
58. Shin Y, Han S, Jeon JS, et al. Microfluidic assay for simultaneous culture of multiple cell types on surfaces or within hydrogels. *Nat Protoc*. 2012;7(7):1247-1259. doi:10.1038/nprot.2012.051
59. Luo X, Wu H-C, Tsao C-Y, et al. Biofabrication of stratified biofilm mimics for observation and control of bacterial signaling. *Biomaterials*. 2012;33(20):5136-5143. doi:10.1016/j.biomaterials.2012.03.037
60. Huh D, Kim HJ, Fraser JP, et al. Microfabrication of human organs-on-chips. *Nat Protoc*. 2013;8(11):2135-2157. doi:10.1038/nprot.2013.137
61. Klingberg TD, Pedersen MH, Cencic A, Budde BB. Application of measurements of transepithelial electrical resistance of intestinal epithelial cell monolayers to evaluate probiotic activity. *Appl Environ Microbiol*. 2005;71(11):7528-7530. doi:10.1128/AEM.71.11.7528-7530.2005

62. Zangmeister RA, Park JJ, Rubloff GW, Tarlov MJ. Electrochemical study of chitosan films deposited from solution at reducing potentials. *Electrochimica Acta*. 2006;51(25):5324-5333. doi:10.1016/j.electacta.2006.02.003
63. Caco-2 [Caco2] ATCC ® HTB-37™ Homo sapiens Colon Colorectal. <https://www.atcc.org/products/all/HTB-37.aspx>. Accessed April 4, 2018.